

Preparation of Mn-doped ZnO nanostructured for photocatalytic degradation of Orange G under solar light

Zahra Barzgari¹ · Ali Ghazizadeh¹ · Seyede Zahra Askari¹

Received: 22 April 2015 / Accepted: 12 September 2015 / Published online: 22 September 2015
© Springer Science+Business Media Dordrecht 2015

Abstract In this study, undoped ZnO and Mn-doped ZnO nanostructured with different doping concentrations were prepared through a facile chemical method. Then, X-ray diffraction (XRD), scanning electron microscopy (SEM), and UV–Vis diffuse reflectance spectra (DRS) techniques were used to characterize the samples. The XRD patterns demonstrated that the synthesized powders had hexagonal wurtzite structure and partial Mn loads on the surface of ZnO. The photocatalytic activities of the samples were investigated by the degradation of orange G solution under sunlight irradiation. The results demonstrated that doping Mn greatly improved the photocatalytic efficiency of ZnO and 6 % Mn-doped ZnO nanostructured exhibited the highest photocatalytic activity under an irradiation time of 1 h. The effect of operating parameters such as amount of catalyst, initial pH, and the initial dye concentration on the rate of dye degradation using 6 % Mn-doped ZnO nanostructured was studied. Under the optimum operation conditions, approximately 94 % dye removal was achieved after 1 h of irradiation.

Keywords Chemical preparation · Nanostructured · Mn-doped ZnO · Photocatalytic performance · Sunlight

Introduction

In recent years, much effort has been devoted to developing highly active heterogeneous photocatalysts for environmental applications, such as air purification, water disinfection, hazardous waste remediation, and wastewater treatment [1–3]. Among various semiconductor metal oxides used in photocatalysis, zinc oxide (ZnO) have attracted extensive research interests because of its non-toxic

✉ Zahra Barzgari
zbarzgari@hotmail.com

¹ Department of Chemistry, Payame Noor University, Birjand, Iran

nature, being strongly oxidizing, low cost, chemical stability, and physical properties [4–6]. However, the application of ZnO semiconductor is limited due to the fast recombination rate of the photogenerated electron–hole pairs [7, 8]. Metal doping is a very useful way to improve ZnO photocatalytic activity, which can act as electron trapping agents to decrease electron hole recombination rates [9]. Xu et al. [10] investigated the relationship between photocatalytic activity of pure ZnO and Co-doped ZnO photocatalysts for the methyl orange (MO) photodegradation. It was found that the photocatalytic properties of the Co-doped ZnO have been greatly improved. The absorption edge shifted to longer wavelengths with the increase of the cobalt concentration. Cd-doped ZnO [11] and Co-doped ZnO [10, 12] indicated better photocatalytic activity than undoped ZnO, due to the increase in oxygen vacancies, as dopants increased. The photocatalytic performance of Ag/ZnO for the degradation of Orange G was evaluated by Lu et al. [13]. Their results indicated that optimized amounts of Ag deposits not only acted as electron sinks to enhance the separation of photoinduced electrons from holes, but also elevated the amount of the surface hydroxyl, leading to the formation of more hydroxyl radicals and then the higher photodegradation efficiency. Mn-doped ZnO has the potential to be a multifunctional material with coexisting magnetic, semi-conducting, and optical properties [14, 15]. Also, it is regarded as a promising material for photocatalytic degradation of dyes [16–20]. Dodd et al. [19] reported the enhanced photocatalytic activity for Mn dopant compared to undoped ZnO under UV- irradiation. Recently, Aris et al. [20] synthesized nano crystalline ZnO particles doped with different concentrations of molybdenum (Mo) and manganese (Mn) (0.2–1.0 %) through the sol–gel method and utilized for photocatalytic degradation of organic pollutants under visible light irradiation. The results indicated that ZnO with dopant concentration of 0.60 % Mo and 0.80 % Mn showed the highest photocatalytic activity as compared to pure ZnO and other dopant concentrations.

The photocatalytic performance of ZnO is closely related to the preparation method and calcination temperature. Recently, a number of techniques such as the sol–gel method [21], the chemical vapor deposition (CVD) method [22], magnetron sputtering [23], the hydrothermal method [11, 24], microwave plasma [25], and the precipitation method [26, 27] have been used for the synthesis of ZnO nanostructures. Compared with the above methods, the precipitation approach provides a facile way for low cost and large-scale production. However, the studies concerning the effect of ZnO morphology and metal doping on its photocatalytic activity are still of great importance and a challenge to explore as they play an important role in determining the extent of their photocatalytic activity [27]. Also, there are few reports about photocatalytic activities of ZnO film under sunlight irradiation.

In this study, we have successfully prepared ZnO and different percents of Mn-doped ZnO nanostructured by a simple chemical method. The photocatalytic activities of the pure and Mn-doped ZnO samples with different doping concentrations for degradation of Orange G (OG) as test contaminants were evaluated under direct sunlight irradiation.

Experimental

Materials and methods

All the chemicals were purchased from Merck and were used without further purification. The typical synthesis procedure for pure and Mn-doped ZnO samples is as follows: $\text{ZnSO}_4 \cdot 7\text{H}_2\text{O}$ (10 mmol) was dissolved into 30 mL of deionized water and ethanol. A suitable amount of $\text{MnSO}_4 \cdot 5\text{H}_2\text{O}$ (the mole ratios of Mn/Zn being 0, 0.03, 0.06, and 0.09) was added to the above solution under vigorous stirring. Then, a known amount of NaOH dissolved in ethanol was added dropwise to the above vigorously stirred solution. After 2 h of stirring, the colloids were dispersed using sonication for 30 min at room temperature. The as-prepared powders were collected by centrifugation, washed several times with deionized water and pure ethanol, and then dried at 70 °C for 4 h.

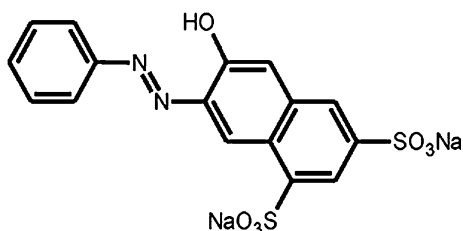
Characterization

The structural characterization of undoped ZnO and Mn-doped ZnO samples was performed using an X-ray diffractometer (XRD, D8 Advance, Bruker) with Cu K α radiation. Morphology and elemental analyses of the samples were performed using Vega Tescan scanning electron microscopy (SEM) which has been equipped with energy dispersive X-ray (EDX) analysis capabilities. A UV–Visible diffuse reflectance spectrum was prepared using an Avantes, model Avaspec-2048-TEC spectrophotometer. The UV–Vis absorption spectra of all samples were taken on a UV–Visible spectrophotometer (PC1601, Shimadzu).

Photocatalytic degradation study

Orange G (OG, $\text{C}_{16}\text{H}_{10}\text{N}_2\text{O}_7\text{S}_2\text{Na}_2$) was used as a model contamination to evaluate the photocatalytic activity of pure and Mn doped-ZnO samples. The structure of the azo dye is shown in Fig. 1. This particular dye (OG) represents one of the mono azo ($-\text{N}=\text{N}-$) dyes that are used in the textile industry, and are subsequently commonly found as water pollutants [28]. All the photocatalytic experiments were carried out at the same conditions in consecutive sunny days and solar light was used as the irradiation source. Approximately 20 mg of photocatalyst was added into 25 mL of an aqueous solution of OG at constant initial concentrations of

Fig. 1 Molecular structure of Orange G dye



10 mg/L. Prior to sunlight irradiation, the suspensions were magnetically stirred in a dark place for 30 min to reach an adsorption/desorption equilibrium for OG on the surface of the photocatalyst. Then the solution was exposed to sunlight irradiation under magnetic stirring. At certain time intervals, 5 mL aliquots were sampled and centrifuged to completely remove the catalyst particles. The effects of the initial pH, initial dye concentration, and the catalyst dosage on the dye degradation were studied in order to achieve maximum degradation efficiency. The concentration of the dye solution was determined by UV–vis spectroscopy. The photodegradation efficiency of OG was calculated using the following equation:

$$\text{Decolorization } \% = \frac{C_0 - C}{C_0} \times 100, \quad (1)$$

where C_0 and C represent the initial concentration of OG prior to irradiation and the concentration of OG after irradiation at certain times, respectively.

Results and discussion

Structural studies

XRD patterns of doped ZnO samples with different Mn doping concentrations and undoped ZnO are shown in Fig. 2. According to the XRD result, all the diffraction peaks match with the standard data for a hexagonal ZnO wurtzite structure (JCPDS 36-1451), and no characteristic peaks from other crystals were detected. So, doped Mn^{2+} ions have no effects on the crystal structure of samples. In addition, negligible changes of all diffraction peak positions and lattice parameters of ZnO in all Mn-doped ZnO photocatalysts compared to that of pure ZnO suggest that the Mn^{+2} dopant ions reside on the surface of the ZnO [13, 29].

The morphologies of the products were investigated by SEM. Figure 3a shows the SEM image of the 6 % Mn-doped ZnO sample. It was clearly seen that particles had spherical morphology with particle diameters in the range of 20–70 nm. The compositional analysis of the 6 % Mn-doped ZnO sample carried out by energy dispersive X-ray analysis is shown in Fig. 3b. The EDX spectrum confirmed the presence of Zn, O, and Mn elements in the sample.

Optical properties

In photocatalytic dye degradation, determination of the band gap of the photocatalyst is necessary. The diffuse reflectance UV–Visible spectra of undoped ZnO and Mn-doped ZnO nanostructured are shown in Fig. 4a. The figure indicates that the reflection rate of the undoped ZnO begins to decrease at 380 nm, while the band edge of the Mn-doped ZnO samples shifted to longer wavelengths. Similar types of behavior have been reported in case of Cd and Co doped ZnO films [10, 11]. In comparison to the undoped ZnO, the absorption edge of the Mn-doped ZnO nanostructured appears remarkably red-shifted indicating a decrease in the band gap

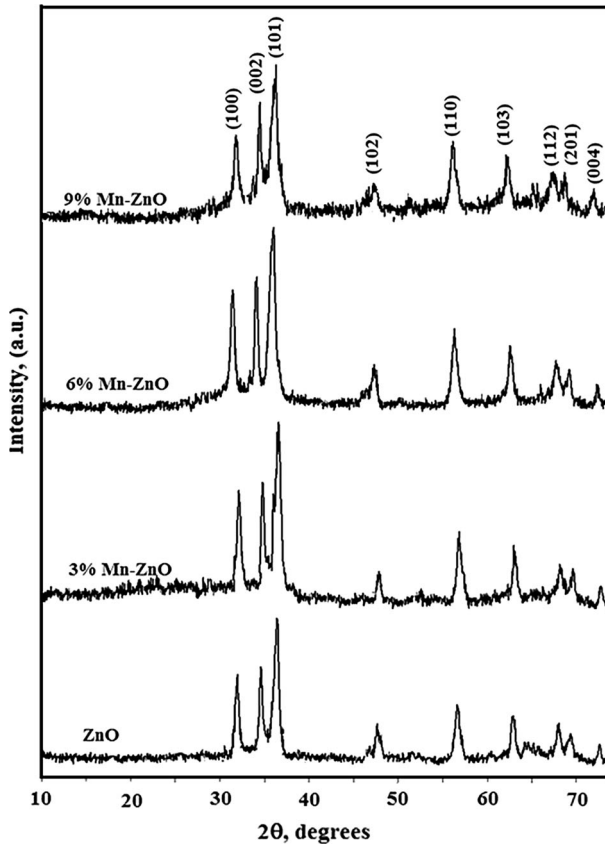


Fig. 2 XRD pattern for undoped ZnO and Mn-doped ZnO samples with different Mn doping concentrations

(see Fig. 4b). The band gap energies of samples were calculated from the diffuse-reflectance spectra by performing a Kubelka–Munk analysis [30, 31]. Figure 4b indicates the band gap energies for all samples as a function of the doping concentrations. With increasing Mn-doped concentration, we can find a decrease in the band gap from 3.34 to 2.60 eV. Gujar et al. [32] reported that the band gap was found to be 3.3 eV for undoped ZnO film and 3.10 eV for Mn-doped ZnO films.

Photocatalytic activity

The photocatalytic behaviors of the undoped and Mn-doped ZnO nanostructured with different amounts of Mn were evaluated by degradation of OG in aqueous solutions under sunlight irradiation. Figure 5a shows the variation in absorption spectra of OG at different time intervals in the presence of 6 % Mn-doped ZnO photocatalyst. The experiments were conducted in a constant dye concentration (10 ppm), catalyst loading (20 mg/L), and 60 min of sunlight irradiation at pH 4. The absorption maximum of the OG dye was found to be at 474 nm. It can be seen

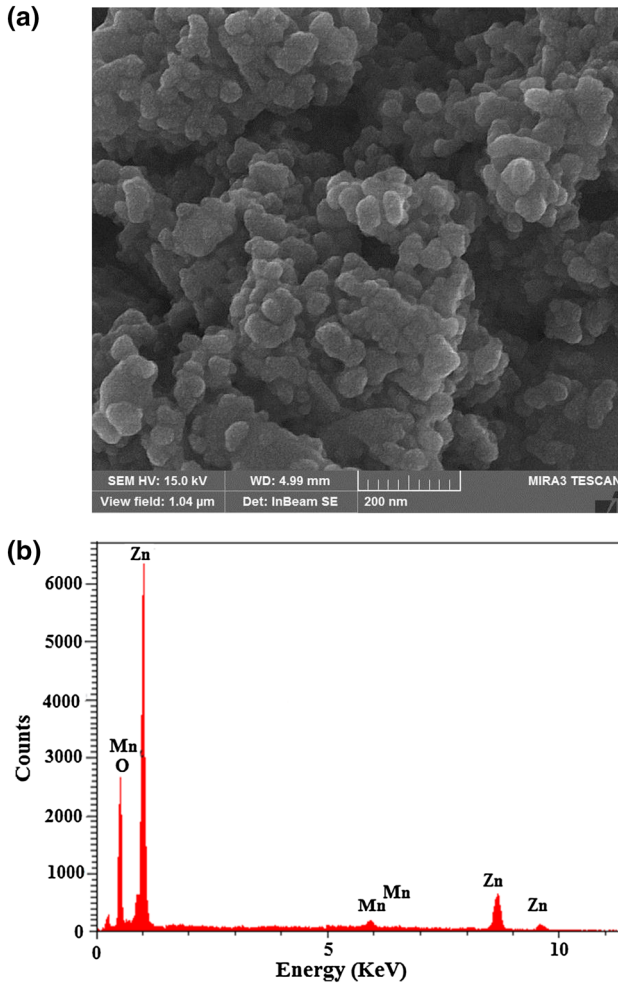


Fig. 3 **a** SEM image and **b** EDX spectrum of 6 % Mn-doped ZnO nanostructured

that the absorption peaks of OG dye gradually decrease with increasing irradiation time. Figure 5b shows the comparison of photocatalytic degradation activity of pure ZnO and Mn-doped ZnO samples. It can be seen from Fig. 5b that all of the Mn-doped ZnO photocatalysts indicated higher photocatalytic performance than the undoped ZnO under same experimental conditions. So, the photocatalytic activity of ZnO can be significantly improved by Mn doping. The positive effect of doping an appropriate amount of Mn is commonly due to the fact that more surface defects could be produced and a space charge layer could be formed on the surface, which is beneficial to improving the separation of photogenerated electrons and holes [33]. The low photocatalytic activity of pure ZnO can be ascribed to the poor charge transport and high recombination rate of photoinduced electrons and holes [2]. It has been observed that photodegradation efficiency was found to increase linearly with

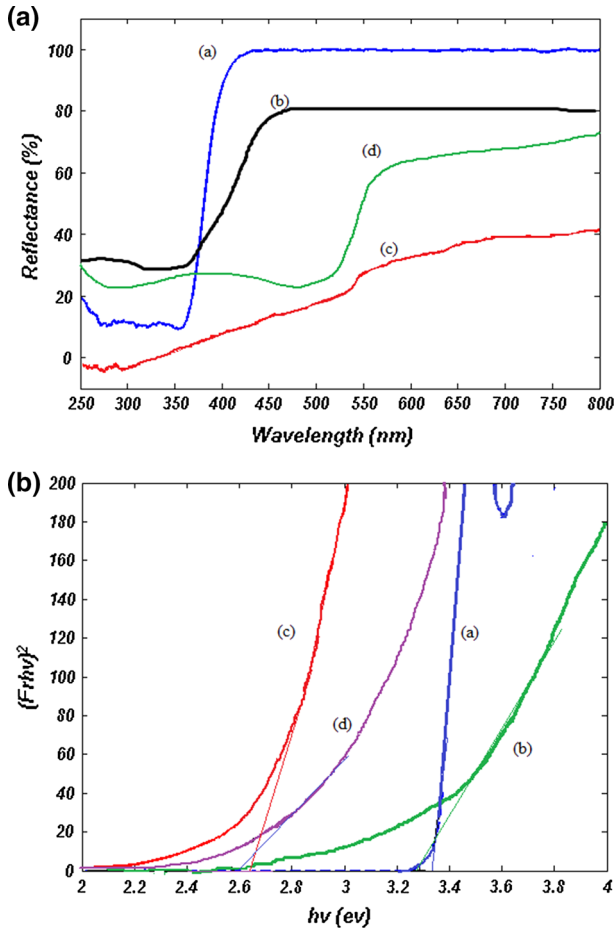


Fig. 4 **a** Diffuse reflectance UV–Visible spectra of undoped ZnO and Mn-doped ZnO prepared with different Mn²⁺ doping concentrations: *a* 0 %, *b* 3 %, *c* 6 %, *d* 9 %, and **b** plot of transferred Kubelka–Munk versus energy of the light absorbed undoped ZnO and Mn-doped ZnO samples *a* 0 %, *b* 3 %, *c* 6 %, and *d* 9 %

increase in Mn contents from 0 to 6 % molar ratio and then declined with further increase of the doping amount. However, when the concentration of Mn⁺² is in excess, the oxygen vacancies and defects would become recombination centers [11, 34]. From the above analysis, it can be concluded that the prepared 6 % Mn-doped ZnO photocatalyst exhibited the highest activity under an irradiation time of 60 min.

Effect of initial concentration of Orang G

The effect of the initial dye concentration on photocatalytic activity of 6 % Mn-doped ZnO nanostructured is shown in Fig. 6. Experiments were performed by

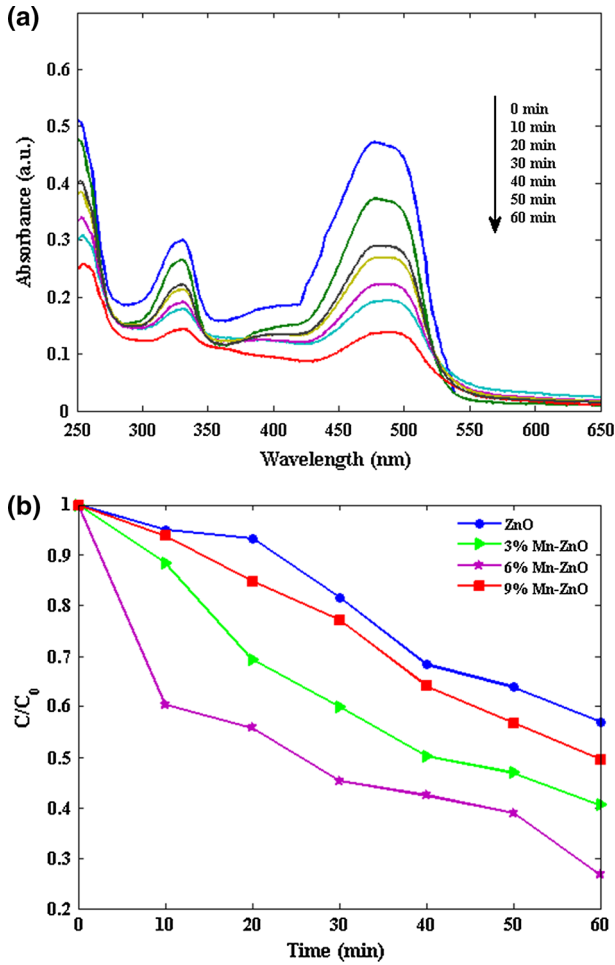


Fig. 5 **a** UV–Vis absorption spectra of aqueous OG solution in the presence of the catalyst 6 % Mn-doped ZnO nanostructured and **b** the comparison of photocatalytic degradation activity of undoped ZnO and Mn-doped ZnO samples with different Mn doping concentrations at pH 4

varying the initial concentration of OG from 5 to 15 ppm in the presence of 20 mg/L of 6 % Mn-doped ZnO nanostructured. As shown in Fig. 6, the photocatalytic activity increased by increasing the dye concentration and then decreased while keeping a fixed amount of catalyst. This may be attributed to reduction in the number of active sites available for the reaction with an increased number of dye molecules at higher dye concentrations [35]. So, the generation of hydroxyl and superoxide radicals at the catalyst surface was reduced since the active sites were occupied by dye. Moreover, as the concentration of dye increased, this also caused the dye molecules to adsorb light with the result that fewer photons could reach the photocatalyst surface and so, photodegradation efficiency decreased [36–38]. Therefore, 10 ppm of OG solution was selected as the optimal concentration of dye for the study of other parameters.

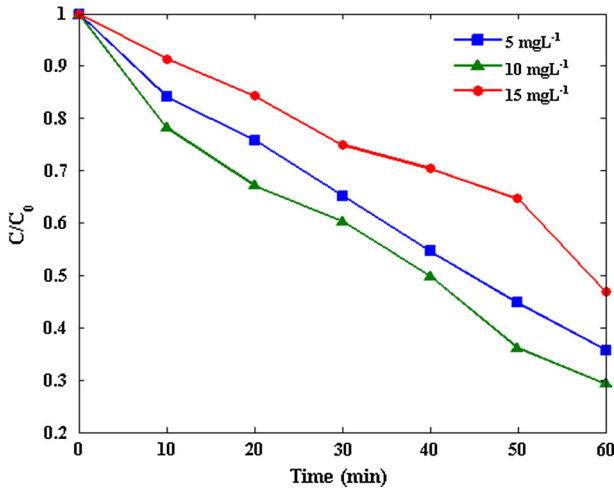


Fig. 6 Effect of initial dye concentration on the degradation of OG under sunlight in the presence of 6 % Mn-doped ZnO nanostructured (pH = 3, time of irradiation = 60 min, catalyst concentration = 20 ppm)

Effect of initial pH

It is well known that pH influences the rate of photocatalytic degradation of some organic compounds [39]. Also it is an important operational variable in practical wastewater. Figure 7 shows the effect of the initial pH, ranging from 3 to 5, on the photodegradation efficiency of 6.0 % Mn-doped ZnO nanostructured. The experiments were conducted in various initial pH values in a constant dye concentration

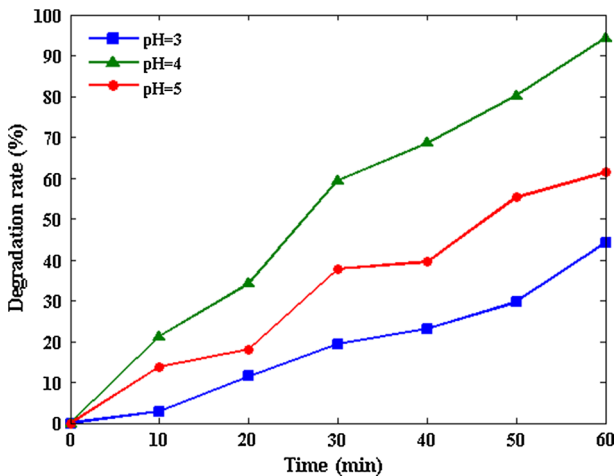
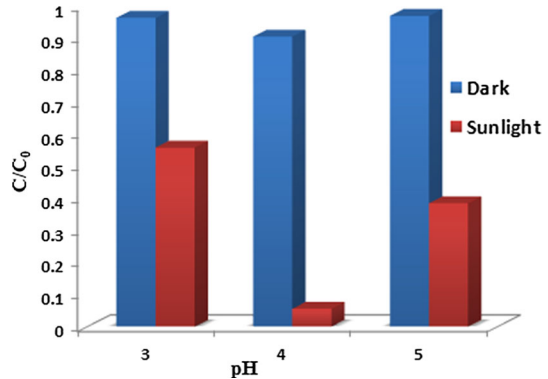


Fig. 7 OG decolorization profiles as a function of irradiation time in the presence of 6 % Mn-doped ZnO nanostructured at different pH under sunlight

Fig. 8 Effect of pH on the degradation of OG under dark and sunlight in the presence of 6 % Mn-doped ZnO nanostructured (time of irradiation = 60 min, initial concentration of dye = 10 ppm)



(10 ppm), catalyst loading (30 mg/L) and 60 min of sunlight irradiation. It is found that a maximum degradation rate of nearly 95 % was obtained at pH 4, while degradation rates of 44.18 and 61.46 % at pH values of 3 and 5, respectively, were obtained after irradiating for 60 min. The OG degradation curves at different pH under dark and sunlight are demonstrated in Fig. 8. The results at pH 4 indicated that about 9 % of the OG was adsorbed by catalyst upon stirring for 30 min in the dark. But, under light irradiation, about 95 % of the OG was degraded. It has been observed that the pH of a solution significantly influences the degradation of OG and 4 was the optimal solution pH. The OG dye in solution is negatively charged as the sulphonated group existing in its structure is hydrolyzed [40]. Due to the electrostatic attraction, the adsorption of OG dye onto the surface of the catalysts is favored in the acidic solution. The photodegradation efficiency decreases with further lowering of the solution pH (below 4.0) due to the dissolution of the 6 % Mn-doped ZnO nanostructured [29, 41, 42]. Evgenidou et al. [42] has reported that the low photocatalytic degradation at a low pH is due to the dissolution of ZnO by measuring the zinc ion in solution at a low pH value. On the other hand, at low pH the concentration of H^+ is in excess, and the H^+ ions interact with the azo linkage, which is particularly susceptible to be electrophilically attacked by a hydroxyl radical, decreasing the electron densities at the azo group [40, 43]. Consequently, the reactivity of a hydroxyl radical by the electrophilic mechanism decreases [43]. Similar results have been reported using TiO_2 in the photodegradation of OG at different pH values [44].

Effect of the dose of photocatalyst

Dye degradation is also influenced by the amount of the photocatalyst. In order to find the optimal catalyst concentration for the photodegradation of OG, a series of experiments were carried out using 6 % Mn-doped ZnO nanostructured under sunlight irradiation. The effect of the dose of photocatalyst on the degradation kinetics of OG was investigated with a 10 ppm dye concentration, pH 4, and catalyst loading in the range of 20–50 mg/L. The results are shown in Fig. 9. It was found that the degradation efficiency increased with an increase in the amount of catalyst to 30 mg/L and decreased with increase in catalyst dosage. This may be due

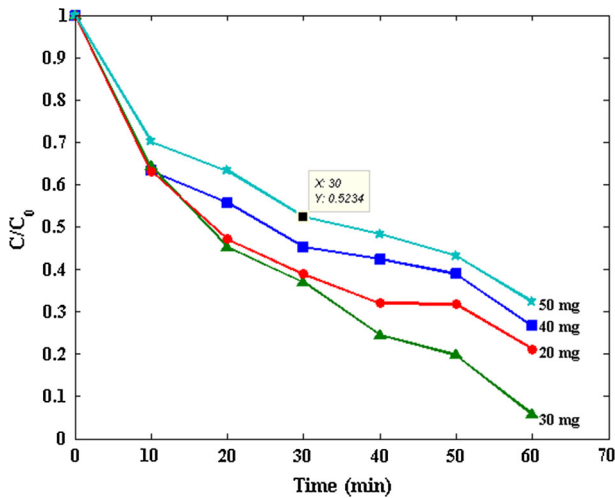


Fig. 9 Effect of catalyst dosage on the degradation of OG under sunlight (pH = 4, time of irradiation = 60 min, initial concentration of dye = 10 ppm)

to an increase in active sites on the surface of the photocatalyst for the reaction, which in turn increases the rate of radical (OH) formation with an increase in catalyst dosage. The reduction in the degradation efficiency beyond 30 mg/L may be due to light scattering and deactivation of activated molecules by collision with ground state molecules [38, 45, 46].

It is well known that the photodegradation rates of organic pollutants on semiconductor surfaces generally follows a pseudo-first-order expression [47]:

$$\ln(C_0/C) = kKt = K_{app} t, \quad (2)$$

where K_{app} is the apparent rate constant, C_0 is the initial concentration of OG in aqueous solution and C is the concentration of dyes at time t . The kinetic rate constants and the degradation efficiency are listed in Table 1. It is clearly seen from Table 1 that the sample indicated the highest value of K_{app} and corresponded to the best photocatalytic activity under sunlight irradiation at 30 mg/L of the photocatalyst. Also, the OG removal percentage is found to be 94.3 % at a photocatalyst loading of 30 mg/L. Thus, 30 mg/L of photocatalyst showed the highest photocatalytic activity for these experiments.

Table 1 Pseudo first order rate constants and percentage degradation of dye solution in the presence of various dosages of catalyst

Catalyst dosages	K_{obs}	% Degradation
20	1.86×10^{-2}	78.9
30	4.23×10^{-2}	94.3
40	2.29×10^{-2}	73.3
50	1.65×10^{-2}	67.6

Conclusion

In this study, undoped and Mn-doped ZnO nanostructured were prepared by the co-precipitation method and were utilized as a photocatalyst on the degradation of OG under sunlight irradiation. The Mn dopant greatly increased the photocatalytic efficiency of the ZnO sample to OG degradation. Several operating parameters were investigated for their further practical application. Maximum dye removal was obtained at an optimum 6 % Mn-doped ZnO nanostructured concentration of 30 mg/L for 10 ppm dye solution at pH 4.

References

1. Z.G. Zou, J.H. Ye, K. Sayama, H. Arakawa, *Nature* **414**, 625 (2001)
2. W.X. Liu, J. Ma, X.G. Qu, W.B. Cao, *Res. Chem. Intermed.* **35**, 321 (2009)
3. H. Farsi, Z. Barzgar, S.Z. Askari, *Res. Chem. Intermed.* (2014). doi:10.1007/s11164-014-1674-x
4. A.A. Ismail, A.A. El-Midany, E.A. Abel-Aal, H. El-Shall, *Mater. Lett.* **59**, 1924 (2005)
5. Y. Du, R.Z. Chen, J.F. Yao, H.T. Wang, *J. Alloys Comp.* **551**, 125 (2013)
6. J. Duan, X. Liu, Q. Han, X. Wang, *J. Alloys Comp.* **509**, 9255 (2011)
7. M.T. Uddin, Y. Nicolas, C.L. Olivier, T. Toupance, L. Servant, M.M. Muller, H.J. Kleebe, J.R. Ziegler, W. Jaegermann, *Inorg. Chem.* **51**, 7764 (2012)
8. S. Anandan, A. Vinu, K.L.P. Sheeja Lovely, N. Gokulakrishnan, P. Srinivasu, T. Mori, V. Murugesan, V. Sivamurugan, K. Ariga, *J. Mol. Catal. A* **266**, 149 (2007)
9. W. Zhang, Z.Y. Zhong, Y.S. Wang, R. Xu, *J. Phys. Chem. C* **112**, 17635 (2008)
10. C. Xu, L. Cao, G. Su, W. Liu, X. Qu, Y. Yu, *J. Alloys Comp.* **497**, 373 (2010)
11. Y.J. Zhai, J.H. Li, X. Fang, X.Y. Chen, F. Fang, X.Y. Chu, Z.P. Wei, X.H. Wang, *Mater. Sci. Semicond. Process.* **26**, 225 (2014)
12. Q. Xiao, J. Zhang, C. Xiao, X. Tan, *Mater. Sci. Eng., B* **142**, 121 (2007)
13. W. Lu, S. Gao, J. Wang, *J. Phys. Chem. C* **112**, 16792 (2008)
14. S. Mondal, S.R. Bhattacharyya, P. Mitra, *Bull. Mater. Sci.* **36**, 223 (2013)
15. S.k. Mandal, T.K. Nath, *Thin Solid Films* **515**, 2535 (2006)
16. B. Donkova, D. Dimitrova, M. Kostadinova, E. Mitkova, D. Mehandjiev, *Mater. Chem. Phys.* **123**, 563 (2010)
17. S. Ekambaram, Y. Iikubo, A. Kudo, *J. Alloys Compd.* **433**, 237 (2007)
18. K. Rekha, M. Nirmala, M.G. Nair, A. Anukaliani, *Phys. B* **405**, 3180 (2010)
19. A. Dodd, A. McKinley, T. Tsuzuki, M. Saunders, *Mater. Chem. Phys.* **114**, 382 (2009)
20. K. Umara, A. Arisa, T. Parveen, J. Jaafar, Z.A. Majid, A.V.B. Reddy, J. Talib, *Appl. Catal. A: Gen.* (2015). doi:10.1016/j.apcata.2015.02.001
21. J. Lu, K. Huang, J. Zhu, X. Chen, X. Song, Z. Sun, *Phys. B* **405**, 3167 (2010)
22. D. Shuang, X.X. Zhu, J.B. Wang, X.L. Zhong, G.J. Huang, C. He, *Appl. Surf. Sci.* **257**, 6085 (2011)
23. C. Besleaga, G.E. Stan, A.C. Galca, L. Ion, S. Antohe, *Appl. Surf. Sci.* **258**, 8819 (2012)
24. Y. Fang, Z. Li, S. Xu, D. Han, D. Lu, *J. Alloys Comp.* **575**, 359 (2013)
25. T. Wangenstein, T. Dhakal, M. Merlak, P. Mukherjee, M.H. Phan, S. Chandra, H. Srikanth, S. Witanachchi, *J. Alloys Comp.* **509**, 6859 (2011)
26. C. Wu, L. Shen, Y.C. Zhang, Q. Huang, *Mater. Lett.* **66**, 83 (2012)
27. N.C.S. Selvam, J.J. Vijaya, L.J. Kennedy, *Ind. Eng. Chem. Res.* **51**, 16333 (2012)
28. P. Modisha, T. Nyokong, E. Antunes, *J. Mol. Catal. A: Chem.* **380**, 131 (2013)
29. Y. Zong, Z. Li, X. Wang, J. Ma, Y. Men, *Ceram. Int.* **40**, 10375 (2014)
30. J.Z. Kong, A.D. Li, H.F. Zhai, Y.P. Gong, H. Li, D. Wu, *J. Solid State Chem.* **182**, 2061 (2009)
31. P.R. Potti, V.C. Srivastava, *Ind. Eng. Chem. Res.* **51**, 7948 (2012)
32. V.R. Shinde, T.P. Gujar, C.D. Lokhande, R.S. Mane, S.H. Han, *Mater. Chem. Phys.* **96**, 326 (2006)
33. T. Jia, W. Wang, F. Long, Z. Fu, H. Wang, Q. Zhang, *J. Alloys Compd.* **484**, 410 (2009)

34. X.C. Song, Y.F. Zheng, E. Yang, G. Liu, Y. Zhang, H.F. Chen, Y.Y. Zhang, *J. Hazard. Mater.* **179**, 1122 (2010)
35. T.G. Venkatesha, Y.A. Nayaka, R. Viswanatha, C.C. Vidyasagar, B.K. Chethana, *Powder Technol.* **225**, 232 (2012)
36. C.C. Wang, C.K. Lee, M.D. Lyu, L.C. Juang, *Dyes Pigment.* **76**, 817 (2008)
37. N. Daneshvar, D. Salari, A.R. Khataee, *J. Photochem. Photobiol. A* **157**, 111 (2003)
38. J. Grzechulska, A.W. Morawski, *Appl. Catal. B* **36**, 45 (2002)
39. C. Wu, X. Liu, D. Wei, J. Fan, L. Wang, *Water Res.* **35**, 3927 (2001)
40. J. Sun, L. Qiao, S. Sun, G. Wang, *J. Hazard. Mater.* **155**, 312 (2008)
41. H.H. Wang, C.S. Xie, W. Zhang, S.Z. Cai, Z.H. Yang, Y.H. Gui, *J. Hazard. Mater.* **141**, 645 (2007)
42. E. Evgenidou, K. Fytianos, I. Poullos, *J. Photochem. Photobiol. A* **175**, 29 (2005)
43. M. Muruganandham, M. Swaminathan, *Dyes Pigment.* **68**, 133 (2006)
44. J. Sun, X. Wang, J. Sun, R. Sun, S. Sun, L. Qiao, *J. Mol. Catal. A: Chem.* **260**, 241 (2006)
45. N. Daneshvar, D. Salari, A.R. Khataee, *Photochem. Photobiol. A* **162**, 317 (2004)
46. K. Byrappa, A.K. Subramani, S. Ananda, K.M. Lokanatha, Rai, R. Dinesh. *Bull. Mater. Sci.* **29**, 433 (2006)
47. C.S. Turchi, D.F. Ollis, *J. Catal.* **122**, 178 (1990)